Full length article

Influence of trap connectivity on H diffusion: Vacancy trapping

Yu Wang [a, b], D. Connétable [b], D. Tanguy [a, *]

[a] Institut Lumière Matière, UMR5306 Université Lyon 1CNRS, Université de Lyon, 69622 Villeurbanne Cedex, France
[b] CIRIMAT, CNRS-INP-UPS UMR 5085, École Nationale d'Ingénieurs en Arts Chimiques et Technologiques (ENSIACET) 4, Alle Émile Monso, BP 44362, F-31030 Toulouse Cedex 4, France

A B S T R A C T

A model is given for the effective diffusion of interstitial solutes in the presence of traps. It goes beyond Oriani's by taking into account, in a simple way, the connectivity between interstitial trap sites. It shows, in particular, that the typical dimension of a network of trap sites, connected by low barriers, appears squared in the diffusion coefficient. Therefore, a large precipitate can be inefficient if it offers a fast diffusion path, even if each individual trap site is deep. The model is illustrated in the case of hydrogen trapping at vacancies in Ni, using ab initio calculations for migration barriers and Kinetic Monte Carlo for validation. Trapping/detrapping kinetic parameters for "Thermal Desorption Spectra" analysis are also given.

Keywords:
Diffusion
Hydrogen embrittlement
ab initio calculation

1. Introduction

Hydrogen trapping plays a key role in the environmental damage of structural metallic alloys. It can be seen from two points of view. Trapping can lead to high H concentrations along potential fracture paths, whether at grain boundaries [1–4] or along intense slip bands [5,6], which lead to H embrittlement. Alternatively, alloy design could be used to enhance trapping away from potential fracture path [7–10], for example, at matrix precipitates instead of dislocations or grain boundaries, opening the possibility to optimize the resistance against H damage. Of particular importance is the role of vacancies. In plasma facing materials for fusion reactors, where H isotopes uptake occurs at the same time as irradiation, vacancy-hydrogen clusters might be at the origin of the formation of bubbles which participate to the deterioration of the surface and also contribute to tritium retention in the material [11,12]. It has also been proposed that such clusters play a direct role in room temperature embrittlement when the vacancies are produced by intense localized plasticity [13,14].

Continuum diffusion equations incorporate trapping [15–17] through an effective diffusion coefficient D_{eff} which reflects the local equilibrium between trap sites and regular interstitial sites in their immediate neighborhood. As shown by Oriani [18], the ratio D_{eff}/D_L (D_L is the diffusion coefficient in the perfect lattice) depends only on the segregation energy ΔE_s and the density of trap sites. Sometimes, the parameters in D_{eff} are misunderstood [19,20] and, indeed, its formulation is not intuitive. First, even if the equilibrium hypothesis is coherent with the absence of any kinetic parameter in D_{eff}/D_L, the absence of any detail concerning the spatial distribution of traps, for example in the case of a trap composed of multiple interstitial sites connected by low energy barriers, is puzzling. Second, it is believed that crystalline defects affect the jump barriers not only in their core but also within a certain radius, creating correlations among H jumps that increase the trap efficiency.

In this paper, we want to discuss these different aspects in the case of the vacancy. The goals are: to derive a physically based model, which contains all the details of the multiple trap [21], show in which conditions Oriani's model is valid and give a methodology applicable to more complex traps, like small precipitates. Furthermore, we choose Ni–H as a model metal-hydrogen system because it is the subject of many experimental and theoretical studies: vacancy-hydrogen clusters are known to be stable [22,23] and have been proposed to play a role in embrittlement [14] (together with other aspects [24,3]), and maybe in oxidation at intermediate temperature [25–27,23]. Therefore, an additional purpose is to give materials specific energy barriers. Such information is also important to model vacancy diffusion in the presence of H [28].

To achieve this, a combination of atomic scale simulations is used: DFT calculations provide material specific jump barriers and "accelerated" Kinetic Monte Carlo (KMC) integrates this information to provide effective diffusion coefficients, taking into account all correlations among jumps. Finally, a semi-analytical model,

* Corresponding author.
E-mail address: dome.tanguy@univ-lyon1.fr (D. Tanguy).

http://dx.doi.org/10.1016/j.actamat.2015.10.018

based on random walk theory and First Passage Time Analysis [29], is derived. It quantitatively reproduces the KMC results and gives a simple picture of trap efficiency which is both a useful guideline for the design of complex traps and an efficient alternative to KMC.

The paper is organized as follows. First, the methods are detailed. Then, the study of diffusion starts with the calculation of the jump barriers for H, inside the vacancy (among the multiple trap sites), and for escaping the vacancy. Then, these data are used to calculate effective diffusion coefficients, as a function of the concentration of vacancies and temperature. The model is used to analyse the results in the discussion section. Its detailed derivation is given in given in the Appendix, together with a discussion of the approximations.

2. Methods

2.1. DFT calculations

The energy barriers for the Ni—H-vacancy system are obtained by first-principles calculations based on the density functional theory (DFT) [30,31], using the Vienna ab initio simulation package (VASP) [32—34]. The generalized gradient approximation (GGA) of the Perdew-Wang (PW 91) form [35,36] for electron-exchange and correlation is used. A plane-wave basis set is employed within the framework of the Blöchl projector-augmented wave (PAW) method [37] to describe the electron—ion interactions. On the basis of a previous work [38], an energy cut-off as large as 400 eV (29.4 Ryd) and a 24 × 24 × 24 Monkhorst-Pack [39] sampling of the primitive Brillouin zone (BZ) are chosen to obtain accurate energy differences. The equilibrium lattice structure is determined by minimizing the Hellmann-Feynman forces on the atoms and the stress on the unit cell. The magnetic moments are taken into account in all calculations. The force convergence criterion is set to 0.01 eV/Å. Two sizes of supercells are tested: 32 and 108 atoms. The differences, with cell size, in segregation energies are less than 0.03 eV. Therefore, the more computationally demanding calculation of the energy barriers for H migration are done on a supercell containing 32 atoms. The Nudged Elastic Band (NEB) method [40] is used to locate the minimum energy pathways (MEP) for hydrogen migration. A spring force-constant of 5 eV/Å is used between images. The convergence of the forces, for each image, is the same as the one for the supercell calculations. In addition to the energy barriers, the "attempt frequency" is also calculated, based only on H vibrations as a first-order approximation of the quantum harmonic transition state theory, as was done previously for bulk diffusion [41]. The frequencies are obtained from the dynamical matrix corresponding to the degrees of freedom of H only. They are such that $h\nu/2k_BT \gg 1$ for T in the 300—600 K range, therefore the vibrational energy can be approximated by the sum of the zero-point energies (zpe): $E_{zpe} = \sum_i 1/2h\nu_i$, where ν_i are the frequencies (real frequencies at the saddle configuration).

2.2. KMC model

Kinetic Monte Carlo [42,43] simulations are used to estimate the H diffusion coefficient in the presence of a vacancy. The time evolution of the system is a series of hops from one interstitial site to a neighboring one. Each hop is independent, and is considered as a Poisson process. The time, in KMC simulations, is given by the constant escape frequency k. k is the sum of the rates corresponding to all possible jump pathways as $k = \sum_j \Gamma_{ij}$, where i is the current state and j is a state connected to i by the jump process. Within the framework of the harmonic approximation of the transition state theory [44,41], the jump rate of a specific path is given by

$$\Gamma_{ij} = \frac{k_BT}{h} e^{-\Delta G_m/k_BT}, \tag{1}$$

where k_B is Boltzmann's constant and h is Planck's constant. ΔG_m is the difference in free energy between the transition state and the ground state, composed of two parts: an electronic energy term ΔE_m (jump barrier) and a vibrational energy term ΔG_{vib} [45,41]. G_{vib} in a periodic structure is, in general, given by

$$G_{vib} = k_BT \sum_i \ln\left[2\sinh\left(\frac{h\nu_i}{2k_BT}\right)\right] \tag{2}$$

where the ν_i are the vibrational frequencies of the system. As discussed above, ΔG_{vib} is approximated by the difference in zpe energy (only the real frequencies are taken into account at the saddle).

At each KMC step, the total jump rate is calculated and the next transition is determined by

$$\sum_{i=1}^{j-1} k_i < rand_1 * k \leq \sum_{i=1}^{j} k_i \tag{3}$$

where $rand_1$ is a uniform random number in (0,1]. Then the increment of time Δt is determined as $\Delta t = -\ln(rand_2)/k$, where $rand_2$ is a second random number between 0 and 1. The interstitial sites inside the vacancy can trap H [46,21]. We will show below that energy barriers within the vacancy are very low with respect to escape barriers. This low-barrier problem precludes KMC simulations from reaching long times. An acceleration method, know as the mean rate method (MRM) [47,29], is used in this situation. More details are given in the KMC section. H on bulk sites is treated with a normal KMC procedure, and H in the basin (vacancy) with the MRM. With the H trajectories obtained by KMC, the diffusion coefficient is measured by the Einstein expression:

$$D = \frac{\left\langle (\vec{r}(t) - \vec{r}(0))^2 \right\rangle}{6t} \tag{4}$$

where $\vec{r}$ is the position of the H atom at t. To get a better statistics, we follow the approach proposed by Kirchheim [48,49], and divide a long trajectory into a number of segments of time length Δt, calculate $D_i = [\vec{r}(i*\Delta t) - \vec{r}((i-1)*\Delta t)]^2/6\Delta t$ and average D_i over the entire simulation duration t to get $D = \sum_i D_i \Delta t/t$. The simulation is long enough so that D does not depend on the chosen Δt.

2.3. Oriani's model

Within the framework of the random walk theory [50,51], the bulk diffusivity D on a cubic lattice is

$$D = \frac{1}{6} n\Gamma l^2 \tag{5}$$

In this expression, n is the number of equivalent jumps (n equals 12 for direct jumps from an octahedral site to another), l is the average jump length ($l = \sqrt{2}/2a_0$, a_0 being the lattice parameter), Γ is the jump rate given by Eq. (1). With the harmonic transition state approximation, D is expressed as

$$D = \frac{k_BT}{h} a_0^2 \exp[-\Delta G_m/k_BT] \tag{6}$$

with ΔG_m, the free energy of activation for a O → O jump. When the tetrahedral interstitial site is sufficiently deep, the diffusion atom temporarily equilibrates in the tetrahedral site [41] and the

diffusion coefficient is:

$$D_L = D \cdot \frac{1}{2}\left(1 + 2e^{-\Delta G_{tet-oct}/k_B T}\right)^{-1} \quad (7)$$

where $\Delta G_{tet-oct}$ is the difference in the free energies for H at the tetrahedral and octahedral sites, and D is given by Eq. (6) with ΔG_m the barrier for a O → T jump.

As briefly mentioned in the introduction, an analytical expression to describe the effect of trapping sites on bulk diffusion of H atom was proposed by Oriani [18]. It was generalized by Kirchheim [48] for multiple-traps in the framework of random walks, in the case of an idealized energy landscape where all saddles have the same energy (but the trap sites have different energies). In this case the jumps are uncorrelated and it can be shown that

$$D_{eff} = D_L \quad 1 + \sum_i \frac{n_i}{n_L} K_i \Big)^{-1} \quad (8)$$

where n_i the number of trap sites of type i, n_L is the number of bulk sites. K_i, the equilibrium constant, is equal to $exp(-\Delta E_s^i/k_B T)$ with ΔE_s^i being the segregation energy of H at trap sites of type i. It is defined as the energy difference of a configuration where H is on site i and the one where H is on a bulk site. o_i is the occupancy of trapping sites of type i. The simulation results will be compared to this model. We will call Eq. (8) "Oriani's model" and it will constitute a reference for KMC simulations and for the new model.

3. H interstitial diffusion and trapping

3.1. H migration barriers: DFT results

H occupies interstitial sites in the fcc lattice of Ni. Our previous calculations [46] show that, in the perfect crystal, the energy is lowered by 0.222 eV when H occupies an octahedral site (O) in comparison to a tetrahedral site (T). The zpe correction enlarges this difference by 0.084 eV, in favor of the O site, in agreement with Wimmer's calculations [41]. The segregation energies on the specific sites of the vacancy (Fig. 1) were also investigated [46]. Segregation is strong on O_1 ($\Delta E_s = -0.273$ eV, including zpe corrections), closely followed by T_1 ($\Delta E_s = -0.222$ eV with zpe) and moderate on O_2 ($\Delta E_s = -0.046$ eV with zpe). Segregation on more remote sites is negligible. In particular, we recall [46] that the ΔE_s profile is oscillating, with a small repulsion on O_3 which is not in favor of the dragging of H atoms towards the vacancy. The study of the "radius of capture" effect will therefore be limited to the study of the influence of O_1, T_1, T_2 and O_2 on the H diffusion coefficient.

Direct jumps between adjacent bulk octahedral sites are not possible, since the energy landscape exhibits a local maximum along this path and not a saddle point [41]. Hence, we consider only migrations through T sites (O-T-O paths). Two pathways are possible for H at O_1 to jump out of the vacancy: $O_1 \rightarrow T_2$ (T_2 is already a bulk site T_b, from the segregation energy point of view, however the barrier to come back to the vacancy is much lower than the one to move away, as shown on Fig. 2) and $O_1 \rightarrow T_1 \rightarrow O_2 \rightarrow T_b$. The relevant values of barriers, evaluated by the NEB, are given in Table 1. The inner barrier $O_1 \rightarrow T_1 \rightarrow O_1$ is very small. Finally, the barrier for the $O \rightarrow T$ jump in the bulk is 0.444 eV, with ZPE correction, which is close to the experimental value (0.43 eV) given by thermal desorption measurements [52].

3.2. KMC-MRM results

With these values of energy barriers, transformed into frequencies by Eq. (1), we perform KMC simulations, first with a simple model containing only O_b and T_b (one O site and 2 T sites per metal atom in the fcc lattice, with the connectivity shown on Fig. 1 of [41]). The diffusion coefficient D_L is in very good agreement with Eq. (7). A fit to the Arrhenius expression $\ln(D) = \ln(D_0) - (Q/k_B)(1/$

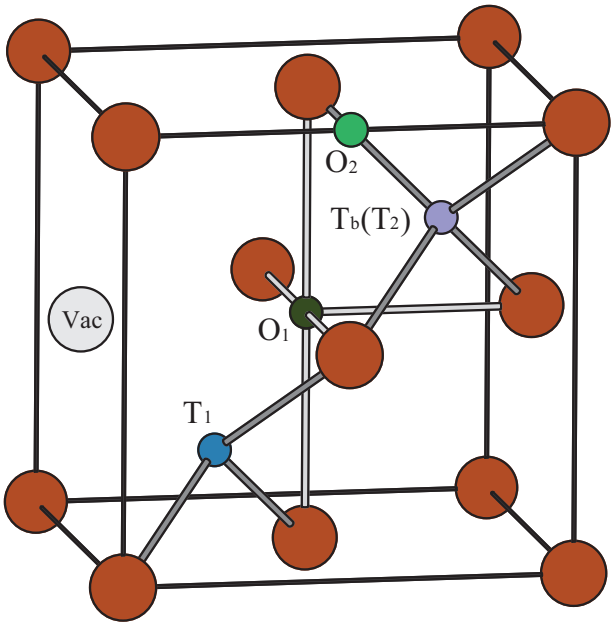

Fig. 1. Schematic representation of the interstitial sites around a vacancy (gray ball) in fcc Ni. O_1 (olive green ball) and O_2 (green ball) are octahedral (O) sites in first and second nearest neighbor (NN) position of the vacancy. T_1 (blue ball) and T_2 (violet ball) are 1NN and 2NN tetrahedral (T) sites. T_2 is already considered as a bulk site, from the segregation point of view (see text).

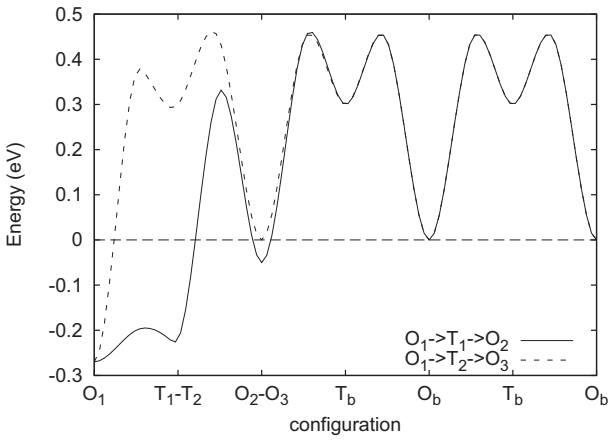

Fig. 2. Energy profile seen by a hydrogen atom in the vicinity of a vacancy. There are two paths to exit the vacancy: one goes through T_1 sites and the other goes through T_2 sites.

Table 1
Jump barriers ΔG_m (eV) (row (initial state) → column (final state)) for H in the vacancy and in the bulk calculated by the NEB method. ZPE corrections are included.

ΔG_m	O_1	T_1	O_2	T_2/T_b	O_b
O_1	–	0.069	–	0.640	–
T_1	0.020	–	0.554	–	–
O_2	–	0.385	–	0.490	–
T_b	0.061	–	0.138	–	0.138
O_b	–	–	–	0.444	–

T), gives a prefactor D_0 of 1.7 $\times$ 10^{-6} m^2s^{-1} and an effective activation barrier Q of 0.48 eV, in good agreement with previous theoretical results (3.8 $\times$ 10^{-6} m^2s^{-1} and 0.47 eV [41]) and experimental works (6.7 $\times$ 10^{-6} m^2s^{-1} and 0.41 eV by Perkins [53] and 4.8 $\times$ 10^{-6} m^2s^{-1} and 0.408 eV reported by Alefeld [54]).

Then the impact of the vacancy is studied. An atom is "removed" from the lattice, i.e. 6 O_1 sites, 8 O_2 sites, 8 T_1 sites and 24 T_2 sites, with the connectivity of the vacancy (Fig. 1) and the jump frequencies corresponding to the barriers of Table 1 are included in the network of O_b and T_b sites used above. The vacancy concentration is adjusted by changing the box size. Only one H atom is considered in the simulation. Therefore, the trapping effect on the diffusion is maximum (we give an upper bound) [55].

From Table 1, the barriers in between O_1 and T_1 are very low (0.069 eV and 0.02 eV) in comparison to the barriers to exit the vacancy (0.64 eV and 0.554 eV). Therefore, a simple KMC is very inefficient since most of the CPU time is spent to simulate inner vacancy jumps. We have noticed that the statistics is so low that we could not recover the equilibrium occupancy of the vacancy, not even after long runs. The Mean Rate Method [29,47] is used to overcome this limitation. The states formed by an isolated H atom occupying one of the 6 O_1 sites or 8 T_1 sites are considered to form a basin of states connected by low barriers ("transient states" in the formalism of absorbing Markov chains [29,47]). There are two different path for a H to exit the vacancy: the jump from O_1 to T_2 (0.64 eV) or the one from T_1 to O_2 (0.554 eV). The states where H occupies T_2 or O_2 sites are the "absorbing states". Having defined the transient and absorbing states, we follow the procedure given in Ref. [29] to select one transition out of the basin and simulate the corresponding waiting time. In such KMC, only one step is necessary to exit the vacancy. We checked that the equilibrium occupancy of the vacancy is recovered after a sufficiently long time is simulated (ergodicity). Note that the correlations related to O_2 and T_2 are preserved. The effect of C_V (the atomic vacancy concentration) and T on H diffusion are studied. The simulated effective diffusion coefficient D_{eff} are presented in Fig. 3. The results are in good agreement with Oriani's model (Eq. (8)), taking into account the vacancy sites O_1,O_2 and T_1 (there is almost no difference if O_2 is ignored), but only at low vacancy concentrations. The trapping effect becomes independent of the vacancy concentration at high C_V.

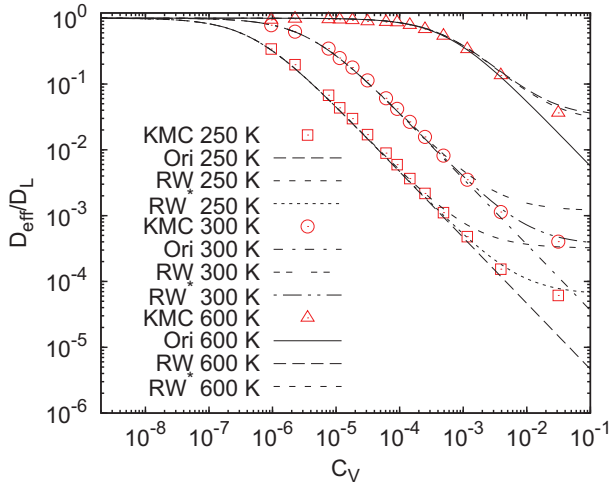

Fig. 3. The ratio of D_{eff} to D_L is given as a function of C_V for three temperatures. KMC simulations (symbols) are compared to two versions of the Random Walk model (RW): first, with O_1 and T_1, only, in the basin ("RW") and, second, with O_1, T_1, O_2 and T_2 in the basin ("RW*"). Oriani's model ("Ori") is also shown.

4. Discussion

We want to analyze the origin of the good agreement between Oriani's phenomenological model and the KMC simulations. For this, a model of D_{eff} is derived from random walk theory (Appendix):

$$D_{eff} = D_{bulk}P_{bulk}\left(1+\frac{\Gamma_{exit}}{\Gamma_{bulk}}\frac{P_{vac}}{P_{bulk}}\frac{\sum_i p_i \Delta\vec{r}_i^{\,2}}{\Delta\vec{r}^{\,2}_{bulk}}\right) \quad (9)$$

$$P_{bulk} = \frac{1+2e^{-\Delta E_s^{T_b}/kT}}{1+2e^{-\Delta E_s^{T_b}/kT}+C_V\left(6e^{-\Delta E_s^{O_1}/kT}+8e^{-\Delta E_s^{T_1}/kT}\right)} \quad (10)$$

D_{bulk} is the diffusion coefficient in the absence of any trap, P_{bulk} (resp. P_{vac}) is the probability for a H to be on a bulk (resp. vacancy) interstitial site (Eq. (10)). Γ_{bulk} is the jump rate from O_{bulk} to O_{bulk}. Γ_{exit} is the average jump rate out of the vacancy. In general, it depends on the entry point and on the internal jump rates, i.e. the jump rates in between the interstitial sites of the vacancy: T_1, O_1 and others, as shown below. $\Delta\vec{r}^{\,2}_{bulk}$ is the squared jump distance relative to Γ_{bulk}, i.e. $1/2a_0^2$. In the case of vacancy jumps, an average is taken over all possible path through the vacancy: $\sum p_i\Delta\vec{r}_i^{\,2}$, where p_i is the probability of path i and $\vec{r}_i$ is the vector connecting the entry and exit sites (i.e. first site in the vacancy and first octahedral site out of the vacancy). The geometrical factor $\sum_i p_i\Delta\vec{r}_i^{\,2}/\Delta\vec{r}^{\,2}_{bulk}$ is called g.

Γ_{exit} is calculated, exactly, by solving the master equations for the occupancies of the interstitial sites inside the vacancy (Appendix). As the inner barriers are low and the network of connected sites has a small dimension, the occupancies reach their equilibrium values before hardly any exit from the vacancy occurs. Therefore Γ_{exit} can be approximated by Γ^{eq}_{exit} (Eq. (A.7)). In this case, g, which depends on temperature and relative trap depth, can be easily calculated ($g \approx 1.8$, see Appendix). It is not much greater than unity for a point defect, but it can be large for other defects like precipitates or dislocation lines, if they offer easy diffusion paths.

The last term to be analyzed is the product $\Gamma_{exit}/\Gamma_{bulk} \times P_{vac}/P_{bulk}$. There is no compensation among the thermally activated terms, contrary to the usual assumption that the activation energy to jump out of the vacancy is $E_a^{exit} = E_a^{bulk} - \Delta E_s$ [12]. Finally, the product scales like $6C_Ve^{0.05/kT}$. At low vacancy concentration, this term is negligible and Eq. (9) reduces to Oriani's model ($D_{eff} = P_{bulk}D_{bulk}$). The result is counter intuitive: the inner sites of the vacancy have the same trapping effect on H whether they are far apart, or connected by low barriers. Indeed, equation (9) shows that, at first order, it is the probability of being on a bulk site which matters for diffusion. It is an equilibrium quantity which does not depend on the details of the escape from the traps. This is valid only if: (i) the density of interstitial trapping sites is low and (ii) these traps are not connected or form networks of small dimensions. In the specific case of the vacancy, C_V has to be pushed high to observe an effect of the connection. The maximum value used for KMC is 3 10^{-2} (Fig. 3). At this concentration, the vacancies are put on a square lattice of dimension 2 a_0. They are sufficiently far apart not to interact. Indeed, the effect of the vacancy is negligible beyond the T_2 site [46] and beyond this distance only bulk sites are considered in KMC. The effect comes from the connectivity in between the 6 O_1, 8 T_1, 8 O_2 and 24 T_2 interstitial sites of the same vacancy.

A quantitative agreement between the model and KMC (Fig. 3) requires O_2 and T_2 sites be taken into account. They have almost no influence on D_{eff} at low C_V (Fig. 3), where all the effect is due to segregation, because the segregation energy on these sites is close to zero ($\Delta E_s^{T_2} = 0$, $\Delta E_s^{O_2} = -0.05$ eV). Nevertheless, O_2 and T_2 play a

large role on Γ_{exit}, and therefore show up at large C_V as shown by the difference between the curves "RW*" and "RW" on Fig. 3 (model with and without O_2 and T_2 respectively, i.e. Eqs. 9 and A.9 versus Eqs. 9 and A.7). The reason is that diffusion jumps starting from O_2 and T_2 are biased: the reduced energy barriers in the direction of the vacancy (Fig. 2) imply jump rates 20 to 70 times higher, at 300 K, in this direction. It brings back H to the vacancy and increase trapping.

Finally, for comparison with thermal desorption spectra [56], Γ_{exit}^{eq} (Eq. (A.9)) is fitted on the Arrhenius form, including the prefactor k_BT/h: the activation energy is 0.69 eV and the pre-exponential factor is 9 10^{13} Hz, slightly different from the values obtained for a single jump [12], from $E_a^{exit} = E_a^{bulk} - \Delta E_s$: 0.74 eV and 10^{13} Hz. Note that the pre-exponential factors used are only valid at low temperature [41] and that lower activation energies for H detrapping are expected for VH_n, due to repulsive H—H interactions.

5. Conclusion

This paper delivers two messages. First, we studied in detail the trapping capacity of vacancies, specifically in Ni, calculating jump frequencies ab initio, for all the relevant paths in and around the vacancy. This information is included in KMC simulations to obtain the H diffusion coefficient. The influence of temperature and vacancy concentration on D_{eff} is well reproduced by Oriani's model, including T_1 and O_1 sites, with multiplicity 8 and 6. This model shows that very high concentrations of vacancies are necessary to have a significant effect on diffusion: beyond 1 ppm at 300 K and beyond 100 ppm at 600 K. These values are orders of magnitude higher than equilibrium VH_n concentrations (i.e. including Fukai's superabundant vacancy effect) which are at maximum of 10^{-15} at 300 K and 10^{-6} at 600 K [23] at very high H concentrations, beyond 1% atomic. Nevertheless, such high vacancy concentrations were reported under very intense localized plasticity conditions [14,57,58].

Second, we model the impact of trap connectivity on H diffusion by deriving Oriani's formula in the framework of random walks and introducing the mean escape frequency from the vacancy. The First Passage Time Analysis from Puchala [29], applied to the basin composed of the states where H occupies the interstitial sites of the vacancy (Appendix), enables a rigorous calculation of the escape frequency with the real connectivity in between the various sites involved. The limitations of Oriani's formula are determined. They have two physical origins. First there is not an exact compensation between the various activation energies involved, namely: the bulk diffusion activation energy, the exit activation energy and the segregation energy. In the case of Ni, this enhances diffusion with respect to Oriani's formula (i.e. the trapping efficiency is lower than predicted by Oriani) below room temperature and at high trap concentration. Second, the trap connectivity is at the origin of a geometric factor which scales like the square of the characteristic length of the network of traps connected by low barriers. It has a weak influence for a point defect but can be important for larger defects, like intragranular precipitates, if they provide long, fast, diffusion paths. The method exposed in the Appendix gives the tools for establishing traps efficiency quantitatively, which can be useful for designing microstructures optimized for resisting to H damage.

Acknowledgments

This work was granted access to the HPC resources of CALMIP (CICT Toulouse, France) under the allocations 2014-p0912 and 2014-p0749. The authors acknowledge the support of the French Agence Nationale de la Recherche (ANR), under grant *EcHyDNA* (Blanc 10-19424). It's a pleasure to thank Danny Perez for discussions about FPTA during visits at LANL, funded by CNRS (PICS program).

Appendix A

D_{eff} is derived from Einstein's formula Eq. (4) [59]. The jumps on regular lattice sites are separated from those which involve the multiple-traps (traps composed of several interstitial sites), for which a mean exit frequency Γ_{exit} is used. In Eq. (4), the position can be written as a sum along a sequence of discrete jumps, that we consider, for the moment, uncorrelated: $\vec{r} = \sum_{n=0}^{N(t)} \Delta\vec{r}_n^2$. The diffusion coefficient becomes:

$$D = \frac{1}{2d} \lim_{N\to\infty} \sum_{n=0}^{N} \frac{\Delta\vec{r}_n^2}{t} \tag{A.1}$$

The sum can be rearranged by grouping the terms that correspond to each specific type of jump, labeled i:

$$D = \frac{1}{2d} \lim_{N\to\infty} \sum_{i} \frac{N_i}{t} \Delta\vec{r}_i^2 \tag{A.2}$$

where N_i is the number of type i jumps among the N jumps and $\Delta\vec{r}_i$ the corresponding jump vector.

Following the general TST, the system evolves by a sequence of transitions in between microstates. A microstate is an energy local minimum in the configuration space of the position of the particles, in particular, H occupying interstitial sites, in the bulk, or in the multiple traps. Following Novotny [60], the microstates which are connected by low energy barriers, i.e. which are frequently revisited by the system, are grouped in a "basin" of states. In the specific case of a single H, trapped in a vacancy composed of several interstitial sites (6 O_1, 8 T_1 etc), the basin is composed of all the microstates obtained by placing the H on the various sites inside the vacancy, i.e. 14 states.

In Eq. (A.2), we separate the jumps that bring the system out the basin, ignore the intra basin jumps, isolate the bulk jumps, and introduce the total time spent in the basin t_{bas} and on bulk sites t_{bulk}:

$$D = \frac{1}{2d} \lim_{N\to\infty} \left(\sum_{i} \frac{N_i}{t_{bas}} \frac{t_{bas}}{t} \Delta\vec{r}_i^2 + \frac{N_{bulk}}{t_{bulk}} \frac{t_{bulk}}{t} \Delta\vec{r}_{bulk}^2 \right) \tag{A.3}$$

$\Delta\vec{r}_i$ is now a vector joining a specific entry site in the vacancy and an exit site (a jump out of the basin, after entrance at a specific site, independent of how precisely the atom visits the inner sites). Now, we introduce N_{bas}, the total number of jumps out the basin:

$$D = \frac{1}{2d} \lim_{N\to\infty} \left(\sum_{i} \frac{N_{bas}}{t_{bas}} \frac{N_i}{N_{bas}} \frac{t_{bas}}{t} \Delta\vec{r}_i^2 + \frac{N_{bulk}}{t_{bulk}} \frac{t_{bulk}}{t} \Delta\vec{r}_{bulk}^2 \right) \tag{A.4}$$

N_{bas}/t_{bas} is the mean exit frequency from the basin (Γ_{exit}), t_{bas}/t is the equilibrium probability of being in the vacancy (P_{vac}) and N_i/N_{bas} is the probability of a specific exit jump that we call p_i, of length $\Delta\vec{r}_i^2$. The bulk part is simply the probability of a bulk jump times the bulk diffusion coefficient that we factorize to isolate a term equivalent to Oriani's model. The final expression is equation (9).

Γ_{exit} is calculated [29] by solving the master equation [61] for the occupancy of the basin states ($o_i(t)$), before first exit:

$$\frac{do_i}{dt} = \sum_j o_j(t)\Gamma_{ji} - o_i(t) \sum_j \Gamma_{ij} - o_i(t) \sum_k \Gamma_{ik}^{exit} \tag{A.5}$$

$$\frac{do_{out}}{dt} = \sum_i \sum_k o_i(t)\Gamma_{ik}^{exit} \tag{A.6}$$

Γ_{ij} is the rate of transition from state i towards j, in the basin (Eq. (1) and Table 1). Γ_{ik}^{exit} is the rate towards state k, out of the basin (exit state, or "absorbing state"). It is not necessary to know the filling of each absorbing state to calculate Γ_{exit}, and therefore they are all grouped in one state, labeled "out" (Eq. (A.6)). There are 15 equations in the case of a vacancy where only sites O_1 and T_1 are considered for constructing the basin. From the o_i, Γ_{exit} can be calculated by Eq. 12 in Ref. [29].

Γ_{exit}^{eq} is a very simple approximation of Γ_{exit} when the barriers in between the states of the basin are low in comparison to exit barriers. In this case, it can be considered that the occupations in the basin follow the equilibrium distribution. The validity of the approximation also depends on the dimension of the basin. In the case of the basin constructed from T_1 and O_1 sites, Γ_{exit}^{eq} is:

$$\Gamma_{exit}^{eq} = \nu\left(4 \times p_{O_1} e^{-\Delta G_{O_1 \to T_b}/kT} + 1 \times p_{T_1} e^{-\Delta G_{T_1 \to O_2}/kT}\right) \tag{A.7}$$

with

$$p_{O_1} = \frac{6e^{-\Delta E_s^{O_1}/kT}}{6e^{-\Delta E_s^{O_1}/kT} + 8e^{-\Delta E_s^{T_1}/kT}} \tag{A.8}$$

and the equivalent for p_{T_1}. The factors 4 and 1 in Eq. (A.7) are the number of exit path from O_1 and T_1 respectively. ν is the frequency k_BT/h. Fig. A.4 shows $\Gamma_{exit}/\Gamma_{exit}^{eq}$ as a function of the $O_1 \to T_1$ jump barrier height and temperature. The approximation is very good in the case of the vacancy, but its quality is problem dependent. A simple validity criterion can be derived by comparing the time for an exit out of the basin (t_{exit}) to the time to visit the states of the basin (t_{eq}). N_{states} is the number of states in the basin. An upper bound for t_{eq} is obtained by supposing that the basin is a linear chain of states, connected by a single barrier ($E_a^{O_1 \to T_1}$ in the case where the basin states involve only the first shell of interstitial sites): $t_{eq} = 2N_{states}^2/\Gamma_{in}$ (one dimensional diffusion). Exit can occur from any state of the basin: $t_{exit} \sim N_{states}/\Gamma_{out}$. The criterion is simply $\Gamma_{in}/\Gamma_{out} \gg 2N_{states}$. At 300 K, with $N_{states} = 14$, it gives $E_a^{out} - E_a^{in} \geq kT\ ln(2 \times 14) \approx 0.077$ eV, in good agreement with Fig. A.4 ($E_a^{in} = E_{O_1 \to T_1} \leq E_a^{out} - 0.077 \approx 0.64 - 0.077 = 0.56$ eV).

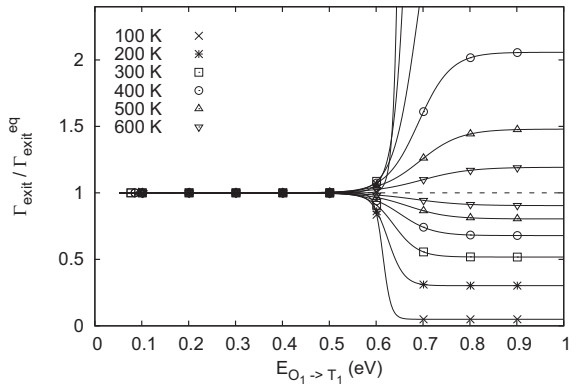

Fig. A.4. Ratio of the mean exit frequency Γ_{exit} (obtained by the First Passage Time Analysis [29]) by the mean exit frequency, in the approximation of an equilibration on the different sites of the vacancy, before H escapes from the vacancy: Γ_{exit}^{eq}.

The geometric term $g = \sum_i p_i \Delta\vec{r}_i^{\,2} / \Delta\vec{r}_{bulk}^{\,2}$ in Eq. (9) can be obtained easily in the case of the vacancy because the equilibrium hypothesis is valid. Let's estimate g in the simple case where O_1 and T_1 only are considered. H can enter the vacancy through T_2 ($T_2 \to O_1$) or through O_2 ($O_2 \to T_1$) with probability 3/4 and 1/4 respectively (this is obtained by calculating the jump frequencies, assuming equilibrium occupancies of O_2 and T_2 and that the jumps barriers towards the vacancy are the same as bulk ones, to simplify). The probability of entering the vacancy at O_1 (resp. T_1) is therefore 3/4 (resp. 1/4). The probability of being on a O_1 site (resp. T_1 site) before exit is $p_{O_1}(T)$ (Eq. (A.8)) (resp. $p_{T_1}(T)$). Finally p_i is the product of these two probabilities. The term $\sum_i p_i \Delta\vec{r}_i^{\,2}$ can be calculated from a list of all possible paths connecting O_1 and T_1 sites. The variation with T is slow in the range 250–600 K, with an average value of 0.91 a_0^2 (a_0 is the lattice parameter of Ni). For a bulk jump, $\Delta\vec{r}_{bulk}^{\,2} = 1/2\ a_0^2$, which gives a ratio $g \approx 1.8$.

Equation (A.7) can be modified when the basin incorporate states corresponding to O_2 and T_2 sites:

$$\Gamma_{exit}^{eq} = 8p_{O_2} \times 5e^{-\Delta G_{O_b \to T_b}/k_BT} + 24p_{T_2} \times 2e^{-\Delta G_{T_b \to O_b}/k_BT} \tag{A.9}$$

where the factors 5 and 2 are the number of paths to leave the vacancy through sites O_2 and T_2 respectively. No migration barriers specific to the vacancy appears anymore, because exit jumps through O_2 and T_2 are bulk jumps. The trapping information is included in p_{O_2} and p_{T_2} (and also in the number of exit paths in Eq. (A.9)):

$$p_{O_2} = e^{-\Delta E_s^{O_2}/k_BT} \Big/ \left(6e^{-\Delta E_s^{O_1}/k_BT} + 8e^{-\Delta E_s^{T_1}/k_BT} + 8e^{-\Delta E_s^{O_2}/k_BT} + 24e^{-\Delta E_s^{T_2}/k_BT}\right) \tag{A.10}$$

A similar expression can be written for p_{T_2}.

References

[1] H. Birnbaum, I. Robertson, P. Sofornis, D. Teter, Mechanisms of Hydrogen Related Fracture – a Review, The Institute of Materials, 1997, p. 172.
[2] R.P. Gangloff, H.M. Ha, J.T. Burns, J.R. Scully, Measurement and modeling of hydrogen environment-assisted cracking in monel k-500, Metallurgical Mater. Trans. A 45A (2014) 3814.
[3] M.L. Martin, B.P. Somerday, R.O. Ritchie, P. Sofronis, I.M. Robertson, Hydrogen-induced intergranular failure in nickel revisited, Acta Mater. 60 (2012) 2739–2745.
[4] D. Di Stefano, M. Mrovec, C. Elsässer, First-principles investigation of hydrogen trapping and diffusion at grain boundaries in nickel, Acta Mater. 98 (2015) 306–312.
[5] H. Birnbaum, P. Sofronis, Hydrogen-enhanced localized plasticity – a mechanism for hydrogen-related fracture, Mater. Sci. Eng. A 176 (12) (1994) 191–202.
[6] I. Robertson, The effect of hydrogen on dislocation dynamics, Eng. Fract. Mech. 68 (6) (2001) 671–692.
[7] J. Takahashi, K. Kawakami, Y. Kobayashia, T. Tarui, The first direct observation of hydrogen trapping sites in tic precipitation-hardening steel through atom probe tomography, Scr. Mater 63 (2010) 261.
[8] J. Takahashi, K. Kawakamia, T. Tarui, Direct observation of hydrogen-trapping sites in vanadium carbide precipitation steel by atom probe tomography, Scr. Mater 67 (2012) 2012.
[9] A. Nagao, M.L. Martin, M. Dadfarnia, P. Sofronis, I.M. Robertson, The effect of nanosized (ti,mo)c precipitates on hydrogen embrittlement of tempered lath martensitic steel, Acta Mater 74 (2014) 244.
[10] F.G. Wei, K. Tsuzaki, Quantitative analysis on hydrogen trapping of tic particles in steel, Metall. Mater Trans. A 37A (2006) 331.
[11] V. Dubinko, P. Grigorev, A. Bakaev, D. Terentyev, G. van Oost, F. Gao, D. Van Neck, E.E. Zhurkin, Dislocation mechanism of deuterium retention in tungsten under plasma implantation, J. Phys. Condens. Matter 26 (2014) 395001.
[12] N. Fernandez, Y. Ferro, D. Kato, Hydrogen diffusion and vacancies formation in tungsten: density functional theory calculations and statistical models, Acta Mater. 94 (2015) 307–318.
[13] M. Nagumo, Hydrogen related failure of steels a new aspect, Mater. Sci. Technol. 20 (2004) 940.
[14] K. Takai, H. Shoda, H. Suzuki, M. Nagumo, Lattice defects dominating hydrogen-related failure of metals, Acta Mater. 56 (2008) 5158.
[15] M. Dadfarnia, P. Sofronis, T. Neeraj, Hydrogen interaction with multiple traps: can it be used to mitigate embrittlement? Int. J. Hydrogen Energy 36 (2011) 10141–10148.
[16] D.N. Ilin, N. Saintier, J.M. Olive, R. Abgrall, I. Aubert, Simulation of hydrogen

diffusion affected by stress−strain heterogeneity in polycrystalline stainless steel, Int. J. Hydrogen Energy 39 (2014) 2418−2422.
[17] P. Sofronis, R.M. McMeeking, Numerical-analysis of hydrogen transport near a blunting crack tip, J. Phys. Mech. Sol. 37 (1989) 317−350.
[18] R. Oriani, The diffusion and trapping of hydrogen in steel, Acta Metall. 18 (1) (1970) 147−157.
[19] L. Ismer, M.S. Park, A. Janotti, C.G.V. de Walle, Interactions between hydrogen impurities and vacancies in mg and al: A comparative analysis based on density functional theory (vol. 80, 184110, 2009), Phys. Rev. B 81 (2010), 139902(E).
[20] D. Araújo, E.O. Vilar, J.P. Carrasco, A critical review of mathematical models used to determine the density of hydrogen trapping sites in steels and alloys, Int. J. Hydrogen Energy 39 (2014) 12194−12200.
[21] R. Nazarov, T. Hickel, J. Neugebauer, Ab initio study of h-vacancy interactions in fcc metals: Implications for the formation of superabundant vacancies, Phys. Rev. B 89 (2014) 144108.
[22] T. Iida, Y. Yamazaki, T. Kobayashi, Y. Iijima, Y. Fukai, Enhanced diffusion of nb in nbh alloys by hydrogen-induced vacancies, Acta Mater. 53 (10) (2005) 3083−3089.
[23] D. Tanguy, Y. Wang, D. Connétable, Stability of vacancy-hydrogen clusters in nickel from first-principles calculations, Acta Mater. 78 (2014) 135−143.
[24] J. Chêne, A. Brass, Role of temperature and strain rate on the hydrogen-induced intergranular rupture in alloy 600, Met. Trans. A 35A (2004) 457.
[25] P. Scott, Mechanisms of intergranular cracking in nickel alloys components of pwrs, in: S. Ishino, B.L. Eyre, J.I. Kimura, INSS (Eds.), Mechanisms of Materials Degradation and Non-destructive Evaluation in Light Water Reactors, 2002, pp. 107−116.
[26] F. Jambon, L. Marchetti, F. Jomard, J. Chêne, Characterisation of oxygen and hydrogen migration through oxide scales formed on nickel-base alloys in pwr primary medium conditions, Solid State Ionics 231 (2013) 69.
[27] M. Dumerval, S. Perrin, L. Marchetti, M. Tabarant, F. Jomard, Y. Wouters, Hydrogen absorption associated with the corrosion mechanism of 316l stainless steels in primary medium of pressurized water reactor (pwr), Corros. Sci. 85 (2014) 251.
[28] Y. Wang, D. Connétable, D. Tanguy, Hydrogen influence on diffusion in nickel from first-principles calculations, Phys. Rev. B 91 (2015) 094106.
[29] B. Puchala, M.L. Falk, K. Garikipati, An energy basin finding algorithm for kinetic Monte Carlo acceleration, J. Chem. Phys. 132 (13) (2010) 134104.
[30] P. Hohenberg, W. Kohn, Inhomogeneous electron gas, Phys. Rev. 136 (1964) B864.
[31] W. Kohn, L. Sham, Self-consistent equations including exchange and correlation effects, Phys. Rev. 140 (1965) A1133.
[32] G. Kresse, J. Hafner, Ab initio molecular-dynamics for liquid-metal, Phys. Rev. B 47 (1993) 558.
[33] G. Kresse, J. Hafner, Ab initio molecular-dynamics simulation of the liquid-metal amorphous-semiconductor transition in germanium, Phys. Rev. B 49 (1994) 14251.
[34] G. Kresse, J. Furthmüller, Efficient iterative schemes for ab initio total-energy calculations using a plane-wave basis set, Phys. Rev. B 54 (1996) 11169.
[35] Y. Wang, J.P. Perdew, Correlation hole of the spin-polarized electron-gas, with exact small-wave-vector and high-density scaling, Phys. Rev. B 44 (1991) 13298.
[36] J.P. Perdew, J.A. Chevary, S.H. Vosko, K.A. Jackson, M.R. Pederson, D.J. Singh, C. Fiolhais, Pair-distribution function and its coupling-constant average for the spin-polarized electron-gas, Phys. Rev. B 46 (1992) 6671.
[37] G. Kresse, D. Joubert, From ultrasoft pseudopotentials to the projector augmented-wave method, Phys. Rev. B 59 (1999) 1758.
[38] D. Kandaskalov, D. Monceau, C. Mijoule, D. Connétable, First-principles study of sulfur multi-absorption in nickel and its segregation to the ni(100) and ni(111) surfaces, Surf. Sci. 617 (2013) 15−21.
[39] H. Monkhorst, J. Pack, Special points for brillouin-zone integrations, Phys. Rev. B 13 (1976) 5188.
[40] H. Jónsson, G. Mills, K. Jacobsen, Classical and Quantum Dynamics in Condensed Phase Simulations, World Scientific, Singapore, 1998.
[41] E. Wimmer, W. Wolf, J. Sticht, P. Saxe, C.B. Geller, R. Najafabadi, G.A. Young, Temperature-dependent diffusion coefficients from ab initio computations: Hydrogen, deuterium, and tritium in nickel, Phys. Rev. B 77 (2008) 134305.
[42] A. Bortz, M. Kalos, J. Lebowitz, A new algorithm for Monte Carlo simulation of ising spin systems, J. Comput. Phys. 17 (1) (1975) 10−18.
[43] D.T. Gillespie, General method for numerically simulating stochastic time evolution of coupled chemical-reactions, J. Comput. Phys. 22 (4) (1976) 403−434.
[44] H. Eyring, The activated complex in chemical reactions, J. Chem. Phys. 3 (2) (1935) 107−115.
[45] A. Van de Walle, G. Ceder, The effect of lattice vibrations on substitutional alloy thermodynamics, Rev. Mod. Phys. 74 (2002) 11−45.
[46] D. Connétable, Y. Wang, D. Tanguy, Segregation of hydrogen to defects in nickel using first-principles calculations: the case of self-interstitials and cavities, J. Alloys Compd. 614 (2014) 211−220.
[47] M. A. Novotny, A Tutorial on Advanced Dynamic Monte Carlo Methods for Systems with Discrete State Spaces, Ch. 3, pp. 153−210.
[48] R. Kirchheim, Monte-carlo simulations of interstitial diffusion and trapping-i. one type of traps and dislocations, Acta Metall. 35 (2) (1987) 271−280.
[49] R. Kirchheim, Hydrogen solubility and diffusivity in defective and amorphous metals, Prog. Mater. Sci. 32 (4) (1988) 261−325.
[50] A.R. Allnat, A.B. Lidiard, Statistical theories of atomic transport in crystalline solids, Rep. Prog. Phys. 50 (1987) 373−472.
[51] D.A. Porter, K.E. Easterling, Phase Transformations in Metals and Alloys, second ed., Chapman & Hall, 1992.
[52] Y. Fukai, Formation of superabundant vacancies in mh alloys and some of its consequences: a review, J. Alloys Compd. 356357 (0) (2003) 263−269.
[53] W.G. Perkins, D.R. Begeal, Permeation and diffusion of hydrogen in ceramvar, copper, and ceramvar-copper laminates, Berichte Bunsenges. Phys. Chem. 76 (8) (1972) 863.
[54] J. Völkl, G. Alefeld, Diffusion of hydrogen in metals, in: G. Alefeld, J. Völkl (Eds.), Hydrogen in Metals I, 28, Springer Berlin Heidelberg, 1978, pp. 321−348.
[55] C. Marte, R. Kirchheim, Hydrogen diffusion in nanocrystalline nickel indicating a structural change within the grain boundaries after annealing, Scr. Mater. 37 (8) (1997) 1171−1175.
[56] C. Hurley, F. Martin, L. Marchetti, J. Chêne, C. Blanc, E. Andrieu, Numerical modeling of thermal desorption mass spectroscopy (tds) for the study of hydrogen diffusion and trapping interactions in metals, Int. J. Hydrogen energy 40 (2015) 3402−3414.
[57] M. Zehetbauer, J. Kohout, E. Schafler, F. Sachslehner, A. Dubravina, Plastic deformation of nickel under high hydrostatic pressure, J. Alloys Compd. 378 (12) (2004) 329−334.
[58] D. Setman, E. Schafler, E. Korznikova, M.J. Zehetbauer, The presence and nature of vacancy type defects in nanometals detained by severe plastic deformation, Mater. Sci. Eng. A 493 (12) (2008) 116−122.
[59] R. Kirchheim, Solid solutions of hydrogen in complex materials, Solid State Phys. 59 (2004) 203−305.
[60] M.A. Novotny, Monte Carlo algorithms with absorbing Markov chains: fast local algorithms for slow dynamics, Phys. Rev. Lett. 74 (1995) 1−5.
[61] S. Ishioka, M. Koiwa, Diffusion coefficient in crystals with multiple jump frequencies, Philos. Mag. A 52 (1985) 267−277.